INSTITUTE OF PHYSICS PUBLISHING JOURNAL OF PHYSICS: CONDENSED MATTER

J. Phys.: Condens. Matter **17** (2005) 3771–3786 doi:10.1088/0953-8984/17/25/005

Optical study of Yb^{3+}/Yb^{2+} conversion in CaF_2 crystals

Sławomir M Kaczmarek[1], Taiju Tsuboi[2], Masahiko Ito[3], Georges Boulon[3] and Grzegorz Leniec[1]

[1] Institute of Physics, Szczecin University of Technology, Aleja Piastów 48, 70-310 Szczecin, Poland
[2] Faculty of Engineering, Kyoto Sangyo University, Kamigamo, Kita-ku, Kyoto 603-8555, Japan
[3] Physical Chemistry of Luminescent Materials, Claude Bernard/Lyon 1 University, UMR CNRS 5620, Bâtiment A Kastler, 10 rue Ampère, 69622 Villeurbanne, France

Received 13 December 2004, in final form 22 February 2005
Published 10 June 2005
Online at stacks.iop.org/JPhysCM/17/3771

Abstract

Yb^{3+} ions with various site symmetries have been observed in the absorption and emission spectra of Yb^{3+}:CaF_2 crystals, both γ-irradiated and annealed in hydrogen. The absorption intensity value is found to be much higher for the γ-irradiated crystal and strongly dependent on the gamma dose. The UV absorption spectra of γ-irradiated and H_2-annealed CaF_2:5 at.% Yb^{3+} crystals are quite similar. Yb^{2+} absorption bands are observed at 360, 315, 271, 260, 227 and 214 nm, which are called A, B, C, D, F and G bands, respectively. For γ-irradiated CaF_2:30 at.% Yb^{3+}, an additional band at 234 nm can be seen. It is suggested that only a negligible amount of Yb^{3+} ions are converted into Yb^{2+} under the γ-irradiation. The presence of Yb^{2+} is confirmed by the 565 and 540 nm luminescence under 357 nm excitation. It is also suggested that the excitation in the A, C, D and F absorption bands of Yb^{2+} gives rise to photo-ionization of Yb^{2+} ions and electrons in the conduction band to form the excited Yb^{3+} ions which emit IR Yb^{3+} luminescence.

The UV absorption and emission spectra obtained for γ-irradiated and H_2-annealed crystals have different structures. This suggests that different mechanisms are responsible for the creation of Yb^{2+} ions. γ-irradiation favours Yb^{2+} isolated centres by reduction of Yb^{3+} ions located at Ca^{2+} lattice sites, whereas annealing in hydrogen favours Yb^{2+} centres neighbouring Yb^{3+} ions when a Yb^{3+} ion pair captures a Compton electron. Also, γ-irradiation does not change the position of Yb^{3+} ions converted into Yb^{2+} in the CaF_2 lattice. In the case of H_2 annealing, a Yb^{3+} ion converted to Yb^{2+} is shifted to the Ca^{2+} position in the lattice.

(Some figures in this article are in colour only in the electronic version)

1. Introduction

Various Yb^{3+}-doped crystals have been investigated and evaluated as candidates for producing a stable laser at 1060 nm in order to replace the conventional Nd:YAG laser [1–4]. Recently, various Yb^{2+}-doped crystals have also been studied with a view to lasers being operated in the visible region [5]. Among many kinds of host materials, CaF_2, which is one of the first materials to be intensively examined for possible lasing [6], has also been used to study the optical properties of both Yb^{3+} and Yb^{2+} ions. The Yb^{3+} ion is interesting because of its strong IR luminescence that can be easily pumped with conventional 940 and 980 nm laser diodes [7–9]. Yb^{2+} doped into CaF_2 is interesting because of its intense and broad yellow-green luminescence [10–12].

In CaF_2 crystal, the Ca^{2+} ion is located at the body centre of a cube of eight F^- ions. As we know from the optical and electron paramagnetic resonance measurements, when trivalent Yb^{3+} is introduced into the crystal, it is substituted for Ca^{2+}, resulting in the creation of Yb^{3+} surrounded by eight F^- ions [13–16]. This replacement by Yb^{3+} gives a contribution to the creation of charge compensation, such as an interstitial F^- ion. Low [13] and McLaughlan and Newman [14] reported that Yb^{3+} ions with trigonal and rhombohedral symmetries are formed, depending on the location of charge-compensating F^-, which is near to Yb^{3+}. If the charge-compensating F^- and impurity ions such as O^{2-} are located far from the Yb^{3+} site, Yb^{3+} with a cubic symmetry is formed. At high dopant concentration (i.e. >0.1 at.%), some kind of structural deformation occurs in the CaF_2 crystal; interstitial F^- ions and vacancies on the normal F^- site compose cuboctahedral clusters. It was observed that in such a cuboctahedral cluster [9], Yb^{3+} ions mainly go to the square-anti-prism site.

In CaF_2 crystal, Yb^{3+} ions with various site symmetries have been observed [9, 15, 17]. The Yb^{3+} ions are initially introduced into the CaF_2 lattice during the process of heating and melting of a mixture of CaF_2 and YbF_3 powders for the crystal growth. The conversion from Yb^{3+} to Yb^{2+} can be undertaken by various methods such as γ-ray irradiation and chemical reduction. It is important to clarify whether Yb^{2+} ions coexist with Yb^{3+} ions in the as-grown crystal and whether Yb^{3+} ions coexist with Yb^{2+} after the conversion. These points have not been clarified so far, and the aim of the present work is to answer these questions.

In the studies of Sm-, Eu-, Tm-doped alkaline-earth fluorides reported in the literature, the conversion from a trivalent rare-earth ion to a divalent rare-earth ion has been undertaken by:

(1) additive coloration under Ca or alkaline-earth metal vapour [18–20];
(2) the electrolytic coloration method [21];
(3) heating the crystal in hydrogen below the melting point [22]; or
(4) irradiation with ionizing radiation, such as γ-rays [23, 24].

In fact, the Yb^{3+} to Yb^{2+} conversion in CaF_2 can be effected by heating the Yb^{3+}:CaF_2 crystal in hydrogen gas at 900 °C [15] and by γ-irradiation [25]. It is not clear whether these conversion methods result in the creation of Yb^{2+} ions with the same site symmetries. In this work, we undertake to effect the Yb^{3+} to Yb^{2+} conversion by two methods, γ-ray irradiation and heating under hydrogen gas, and will make an attempt to clarify what kinds of Yb^{2+} centres are created.

2. Experimental details

$Ca_{1-x}Yb_xF_{2+x}$ ($x = 0.005$, 0.02, 0.05, 0.15 and 0.3) crystals were prepared at the Tohoku University, Japan [9], by simply melting mixtures of commercially available powders of CaF_2 and YbF_3 with the purity of 4N. The furnace was driven with a 30 kW RF generator and a

carbon crucible was used for melting materials. The furnace was evacuated to 10^{-4} Torr prior to the synthesis to eliminate oxygen and/or water, and then CF_4 gas was slowly introduced. The melting was performed under CF_4 atmosphere. After the materials were completely melted, the furnace was slowly cooled down to room temperature.

The crystals obtained were transparent colourless crystals. Their size was a few centimetres, but actually they were polycrystals consisting of some grains and cracks. Each grain was quite large, from a few mm to a few cm, so we could assume that the quality was as high as that of a single crystal.

The crystals were irradiated with γ-rays at room temperature in the Institute of Nuclear Chemistry and Technology, Poland, with doses varying from 10^4 to 10^5 Gy, and annealed in hydrogen at 1323 K for 1 h (with the growth rate of 6 °C min^{-1}) in the Institute of Electronic Materials Technology, Poland. In order to determine the influence of γ-quanta and the annealing in hydrogen on the absorption spectra, room temperature transmission measurements were performed in the Institute of Optoelectronics, MUT, Poland, using Lambda-900 and FTIR-3025 spectrophotometers. The additional absorption coefficient of a given sample after gamma irradiation was calculated from the formula

$$\Delta K = \frac{1}{d} \ln \frac{T_1}{T_2}, \tag{1}$$

where d denotes the sample thickness, and T_1 and T_2 are transmissions of the sample before and after a given treatment. Pure CaF_2 single crystals were subjected to gamma exposure to compare the influence of γ-quanta on the absorption spectrum with that of the Yb^{3+}-doped crystals.

Unpolarized absorption spectra were measured with a Cary-5E spectrophotometer in the spectral range of 190–3100 nm at temperatures from 16 to 300 K for both 'as-grown' and γ-irradiated CaF_2:Yb^{3+} (30 wt%) crystals at the Kyoto Sangyo University, Japan. The spectral resolution was set at 0.2 nm. Absorption measurements have also been performed at the Lyon 1 University [9], France.

Photoluminescence measurements were carried out for the 'as-grown', hydrogen-annealed and γ-irradiated crystals using an SS-900 Edinburgh Inc. spectrophotometer in the Institute of Optoelectronics, MUT, Poland. Emission measurements have also been made at the Lyon 1 University [9], France.

Electron spin resonance (EPR) measurements were carried out using a Bruker E500 electron paramagnetic resonance spectrometer working in the microwave x-band (∼9.5 GHz). An additional liquid helium flow cryostat produced by Oxford Instruments with a temperature controller enabling temperature variable studies of samples in the 3.5–350 K range was also used. The oriented sample was previously γ-irradiated and then annealed in air for 3 h.

3. Experimental results

Figure 1 shows the room temperature absorption spectra of the 'as-grown' CaF_2 crystals with 0.5 and 5 at.% Yb^{3+} ions and a spectrum of the CaF_2:5 at.% Yb^{3+} crystal heated in hydrogen gas at 1323 K for one hour. All 'as-grown' samples show the same Yb^{3+} absorption line shape in the 900–1150 nm region, while the H_2-annealed crystal reveals some new absorption bands below 400 nm in addition to the IR absorption band. The absorption bands are observed at 360, 315, 271, 260, 227 and 214 nm, and are called A, B, C, D, F and G bands, respectively. The B band is the weakest one and the G band is observed as a shoulder of the F band. Such UV absorption bands have been observed by several investigators and were attributed to Yb^{2+}-and Yb^{2+}-associated centres [25–28] in various host materials [29, 30].

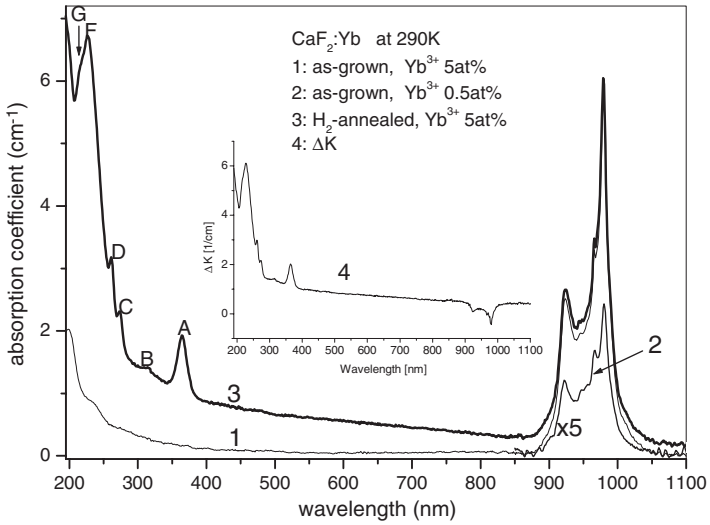

Figure 1. Room temperature absorption spectra of the 'as-grown' CaF_2 crystals with 0.5 and 5 at.% Yb^{3+} ions (curves 2 and 1, respectively) and CaF_2:5 at.% Yb^{3+} crystal heated in hydrogen gas at 1323 K for one hour (curve 3). Curve 2 is five-times enlarged. Curve 4, shown in the inset, shows the additional absorption (ΔK) of CaF_2:5 at.% Yb^{3+} after annealing in hydrogen.

In the inset of figure 1, one can see an additional absorption band that, beside the above-mentioned Yb^{2+}-related bands, reveals a decrease in the range of Yb^{3+} IR absorption after annealing in hydrogen. This decrease was confirmed by luminescence measurements showing lower luminescence in the 900–1100 nm range in the crystal after annealing in hydrogen.

Figure 2 shows the UV absorption spectra of 10^5 Gy γ-irradiated CaF_2 crystals with 5 and 30 at.% Yb^{3+} ions at 18 and 288 K. It can be seen that besides the A–G absorption bands, an additional band appears at 234 nm for γ-irradiated CaF_2:30 at.% Yb^{3+}. It is called the E band. Unlike the case for H_2-annealed CaF_2:5 at.% Yb^{3+} crystal, we notice that the B band intensity is almost comparable to that of the A band. Also, the G band of the γ-irradiated CaF_2:30 at.% Yb^{3+} crystal is much wider than the F band. Except for the intensity value, which is much higher for γ-irradiated crystal, the UV absorption spectrum of the γ-irradiated CaF_2:5 at.% Yb^{3+} crystal is quite similar to that of the H_2-annealed crystal. With decreasing temperature, the B band shifts towards higher energy, while the other bands remain at their positions (see also figure 3). The intensity ratio of the A, B and G bands depends on the Yb^{3+} concentration and the method of $Yb^{3+} \rightarrow Yb^{2+}$ conversion, while the intensity ratio (integrated area) of the A, C, D and F bands does not show such a dependence (is almost constant, i.e. 1.0:0.7:1.1:4.1).

Comparing the insets of figures 2 and 1, one can see that no one additional absorption band is present for the γ-irradiated crystals in the range 900–1100 nm. This observation has been confirmed by luminescence measurement and it suggests that only a negligible amount of Yb^{3+} ions are converted into Yb^{2+} under the influence of γ-irradiation. However, this amount is enough to yield large changes in the Yb^{2+} absorption spectrum below 400 nm.

Moreover, the different structure of the UV spectrum of γ-irradiated crystals compared with the spectrum of annealed-in-hydrogen crystals suggests that different mechanisms are responsible for the creation of Yb^{2+} ions.

The intensity of Yb^{2+} absorption after γ-irradiation strongly depends on the irradiation dose. As can be seen in figure 2(a), an increase in the irradiation dose from 10^4 to 10^5 Gy leads to almost twice as large an increase in the additional absorption value. This was observed for

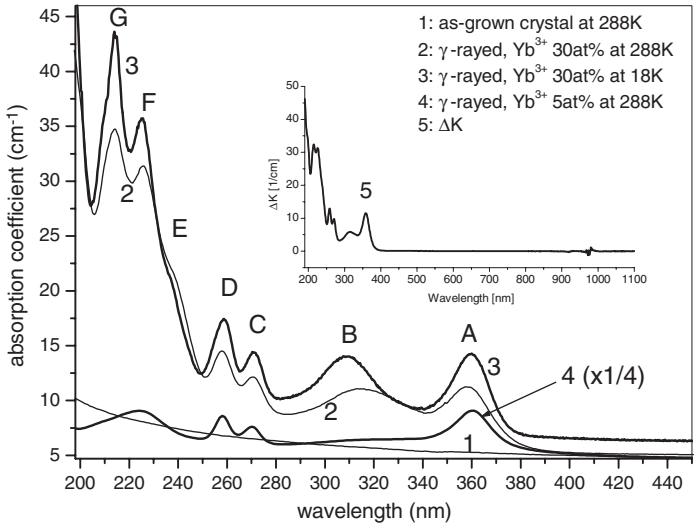

Figure 2. Absorption spectra of the 10^5 Gy γ-irradiated CaF_2 crystals with 5 and 30 at.% Yb^{3+} ions at 18 K (curve 3) and 288 K (curves 4 and 2, respectively), and an absorption spectrum of 'as-grown' CaF_2 crystal with 30 at.% Yb^{3+} ions at 288 K (curve 1). The inset presents an additional absorption after γ-irradiation (ΔK) (curve 5).

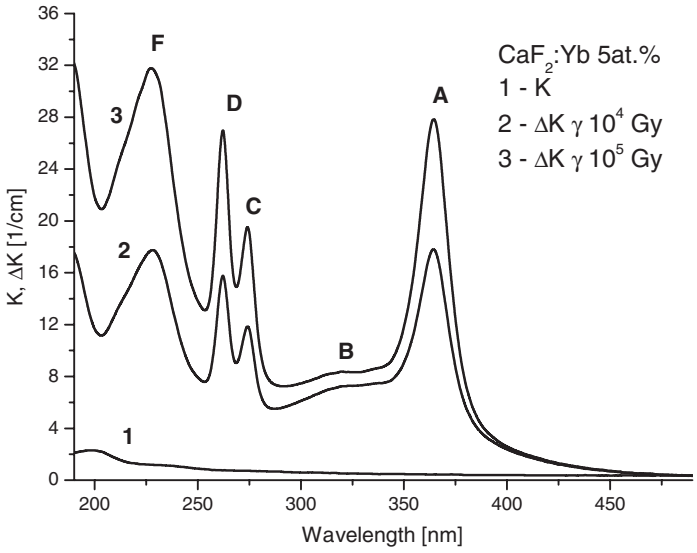

Figure 2a. Absorption (1) and additional absorption of the CaF_2:Yb^{3+} 5 at.% crystal after γ-irradiation with a dose of 10^4 Gy (2) and 10^5 Gy (3).

the A, C, D and F bands, but not for the B band. Therefore it is concluded that the A, C, D and F bands have an identical Yb^{2+} origin, while the B, E and G bands have another origin.

As shown in figure 3, all the bands become sharp and narrow with decreasing temperature. Therefore, the absorption band area is almost unchanged under variation of temperature, indicating that these bands are not due to dipole forbidden and vibration-induced transitions but due to dipole allowed transitions.

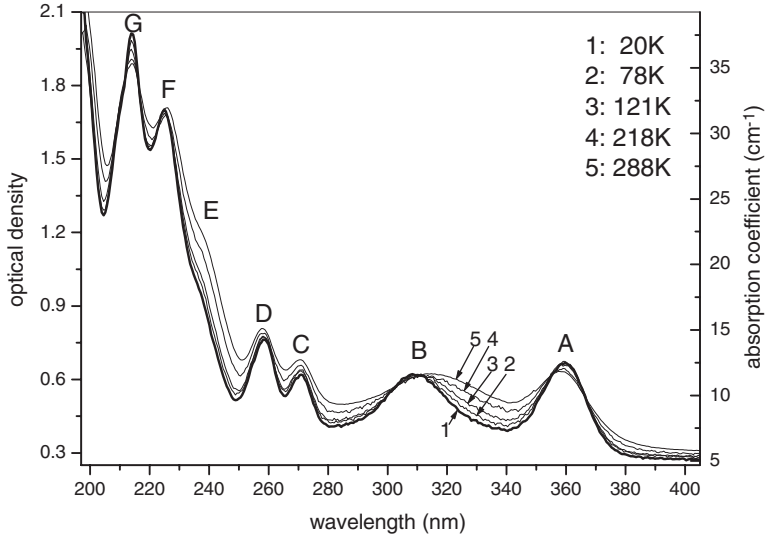

Figure 3. Temperature dependence of the UV absorption bands in 10^5 Gy γ-irradiated CaF_2:30 at.% Yb^{3+} crystal.

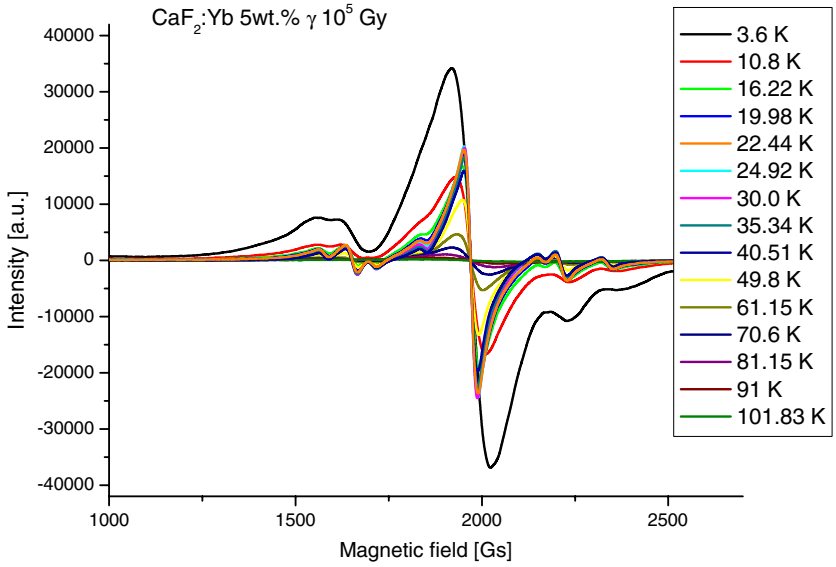

Figure 4. The temperature dependence of the EPR spectra of γ-irradiated CaF_2:5 at.% crystal.

Figure 4 shows the temperature dependence of EPR spectra of γ-irradiated CaF_2:5 at.% crystal. The EPR signal consists of eight lines centred at $g = 4.293, 4.1, 3.965, 3.665, 3.443, 3.13, 3.054$ and 2.894. It is observed that the EPR signal appears at low temperature below about 102 K and decreases with increasing temperature. Figure 5 shows the temperature dependence of EPR spectra of CaF_2:Yb 5 wt% crystal annealed at 400 °C for 3 h after γ-irradiation. The EPR line shape is not changed by the annealing. The signal decreases with increasing temperature as in the case of figure 4. Figure 6 shows the comparison between the

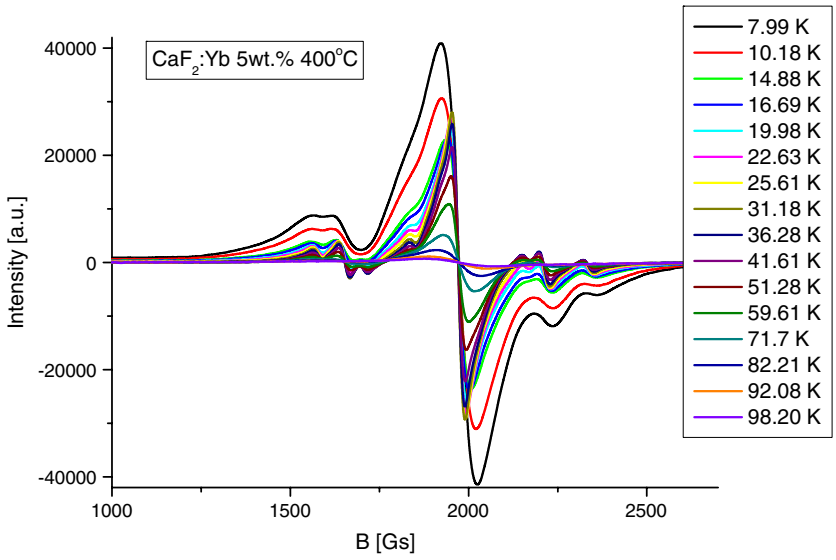

Figure 5. The temperature dependence of the EPR spectra of CaF_2:Yb 5 wt% crystal annealed at 400 °C for 3 h after γ-irradiation.

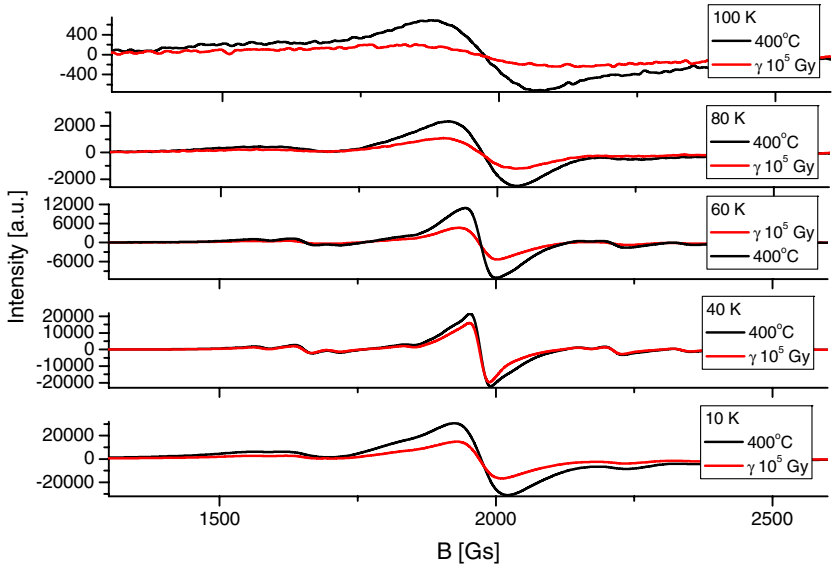

Figure 6. The comparison between the EPR signals of the annealed CaF_2:5 at.% crystal after and before γ-irradiation.

EPR signals of the annealed CaF_2:5 at.% crystal after and before γ-irradiation. It is observed that the EPR intensity decreases upon γ-irradiation.

Figure 7 shows the IR absorption spectra of γ-irradiated CaF_2:30 at.% Yb^{3+} crystal at various temperatures. At 18 K, absorption bands are observed at 922.5, 942.7, 963.0, 977 nm. They are called Y1, Y3, Y4 and Y5 bands, respectively. We can see that the Y3 band has a side band on the low energy side (at 948 nm), and the Y4 band has a weak band at about 960

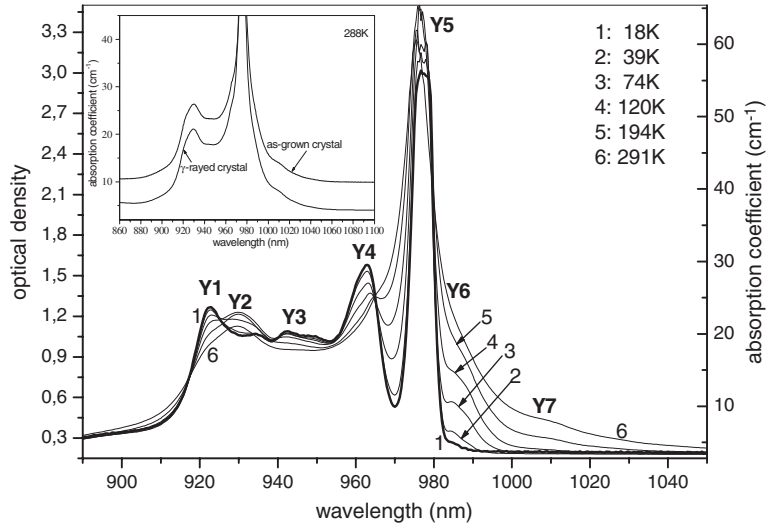

Figure 7. Temperature dependence of the IR absorption bands of 10^5 Gy γ-irradiated CaF_2:30 at.% Yb^{3+} crystal. Comparison with the IR spectrum of as-grown CaF_2:30 at.% Yb^{3+} crystal at 288 K is shown in the inset.

nm. The exact peak height of the Y5 band is not clear because it is so intense (see figure 1) that luminescence arising from the excitation with the Y5 band itself appears and deforms the absorption line shape. With increasing temperature, the intensities of the Y1 and Y3 bands decrease, while the Y4 band shifts to lower energy, up to 965 nm at 291 K, and new absorption bands appear at 930, 984.7 and about 1007 nm. These bands are called Y2, Y6 and Y7, respectively.

Such temperature-sensitive bands have been observed on the low energy side of the intense absorption band for various crystals doped with rare-earth ions, and are attributed to the hot bands [31–33]. Hot bands are caused by transitions from thermally populated upper levels in the $^2F_{7/2}$ ground state that are split by the crystal field to the $^2F_{5/2}$ state, also split by the crystal field. We observed a sharp Y4 band at 963.0 nm attended by a 960 nm band at low temperatures. This band is attributed to cubic Yb^{3+} by Kirton and McLaughlan [15] and to the $1 \rightarrow 6$ transition of the cuboctahedral site by Ito *et al* [9].

The Y2 band is broad (like Y3) and increases with increasing temperature. It is therefore attributed to a phonon side band as is confirmed in figure 8 for low Yb^{3+} concentration (0.5%) [9]. The inset of figure 7 shows the IR absorption spectra of the as-grown and γ-irradiated CaF_2:30 at.% Yb^{3+} crystals at 288 K. No difference is observed between the two crystals.

Figure 9 shows the room temperature absorption spectra of a pure CaF_2 crystal (i.e. crystal where no impurity, including Yb^{3+}, is introduced) before and after γ-irradiation. Several very weak absorption bands can be seen in the visible region for the γ-irradiated crystal. The most intense band is observed at 376 nm and it is attributed to the absorption due to F colour centres (i.e. negative ion vacancies trapping electrons) [34].

The H_2-annealed CaF_2:Yb^{3+} crystals reveal luminescence bands in the 950–1100 nm region upon excitation with UV light. Figure 10 shows the room temperature luminescence spectrum of the CaF_2:5 at.% Yb^{3+} crystal excited with 261 nm light. This luminescence spectrum consists of three bands at 980, 1013 and 1030 nm. The same spectrum was obtained by

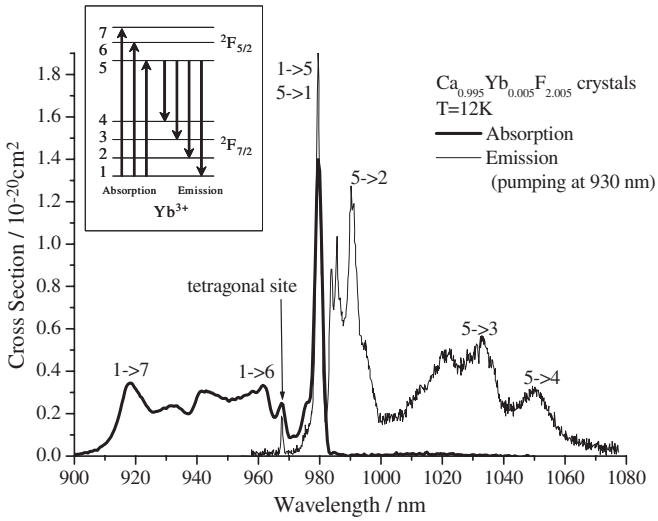

Figure 8. Absorption and emission spectra at 12 K of CaF_2 crystal containing 0.5 at.% Yb^{3+}. The emission spectrum was obtained by excitation with 930 nm light. The inset shows the electronic transitions for the observed absorption and emission bands.

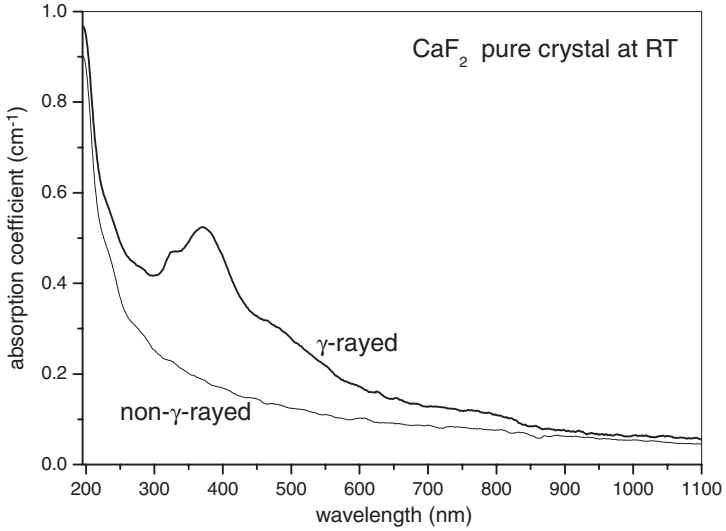

Figure 9. Room temperature absorption spectra of CaF_2 crystals containing no Yb^{3+} ions before and after 10^5 Gy γ-ray irradiation.

excitation with 226 and 273 nm wavelengths. Figure 10 also shows the excitation spectrum for 980 nm emission, indicating that the absorption band at 234 nm gives rise to IR luminescence. The same IR luminescence bands are produced by excitation of γ-irradiated crystal. The excitation spectrum for 980 nm emission is shown in figure 11. Several excitation bands can be seen with almost the same peak positions as the A, C, D, E and F absorption bands, although the peak height ratio is different from that for the absorption spectra of figure 2.

The inset of figure 11 shows the luminescence spectra of three types of CaF_2:5 at.% Yb^{3+} crystal: 'as-grown' crystal, H_2-annealed and γ-irradiated, excited with the 920 nm wavelength.

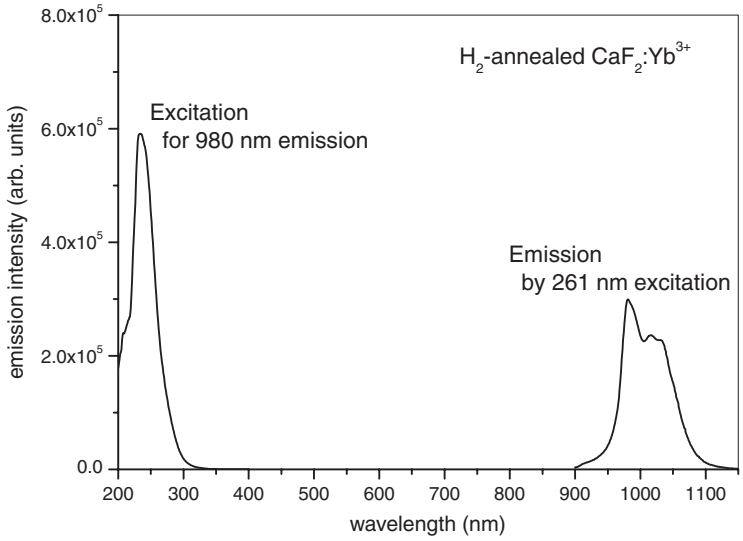

Figure 10. Room temperature excitation spectrum for 980 nm emission of CaF_2:5 at.% Yb^{3+} crystal heated in hydrogen gas at 1323 K for one hour and its luminescence spectrum obtained by excitation with 261 nm light.

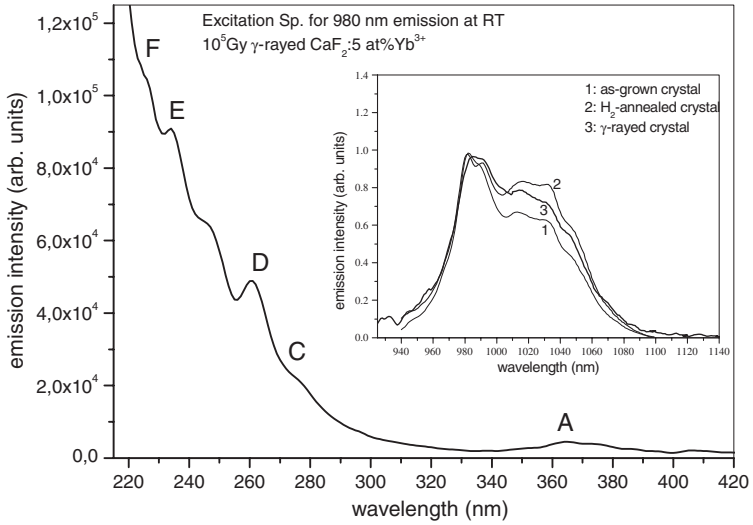

Figure 11. Room temperature excitation spectrum for 980 nm emission of 10^5 Gy γ-irradiated CaF_2:5 at.% Yb^{3+} crystal. The Inset shows the normalized-to-1 luminescence spectra of three types of CaF_2:5 at.% Yb^{3+} crystal: (1) 'as-grown' crystal, (2) heated in hydrogen gas at 1323 K for one hour, (3) 10^5 Gy γ-irradiated, excited with 920 nm light.

We can see a difference in intensity ratio among the 980, 1013 and 1030 nm emission bands in the spectra of these three different crystals.

We have also obtained the room temperature luminescence spectrum of γ-irradiated CaF_2:30 at.% Yb^{3+} crystal excited with the 357 nm wavelength (357 nm excitation means excitation of the A absorption band). Very weak emission bands were observed at about 565 and 535 nm, overlapping each other.

4. Discussion

4.1. The presence of Yb^{3+} ions in as-grown crystals

The A–G UV absorption bands related to Yb^{2+} ions are not observed for the 'as-grown' CaF_2 crystals doped with YbF_3, and in the IR region only the trivalent Yb^{3+} absorption bands appear. This indicates that Yb^{2+} ions are not present in 'as-grown' crystals. Scacco *et al* [35] reported that, in 'as-grown' $KMgF_3$ crystals doped with YbF_3 containing Yb^{3+} ions, only Yb^{2+} ions are created without any reduction procedure and Yb^{3+} ions are not present. The same was observed for 'as-grown' $KMgF_3$ crystals doped with $EuBr_3$ or $EuCl_3$, where divalent Eu^{2+} ions are created and trivalent Eu^{3+} ions are not present [35–37]. Why does such a difference occur between the 'as-grown' CaF_2 and $KMgF_3$ in spite of the fact that a powder containing trivalent rare-earth ions is added in the growing process for both samples? This can be explained as follows.

$KMgF_3$ crystal belongs to the O_h space group with the cubic unit cell where a K^+ ion is surrounded by twelve F^- nearest neighbours forming a cuboctahedron and a Mg^{2+} ion is placed at the centre of octahedron composed of six F^- ions. The ionic radius of K^+ in the twelvefold coordination is equal to 0.178 nm, while the Mg^{2+} ion has a smaller ionic radius of 0.086 nm in the sixfold coordination [38]. The ionic radii of Eu^{2+} (0.149 nm) and Eu^{3+} (0.120 nm) are smaller than the K^+ radius but larger than the Mg^{2+} one. Thus, it is more likely that the Eu^{3+} and Eu^{2+} ions are substituted for the K^+ ions. This gives rise to the formation of charge-compensating positive ion vacancies located at K^+ sites [36, 39].

As is well known, for the substitution of Eu^{3+} and Eu^{2+} ions for monovalent K^+, two and one vacancy are necessary, respectively. It is suggested that the Eu^{2+} substitution is more favourable than the Eu^{3+} one, because the host $KMgF_3$ is not favourable for the creation of a large number of vacancies and for the large valence difference between guest and host ions. During melting of the mixture of KF, MgF_2 and $EuCl_3$ (or $EuBr_3$) powders, only Eu^{3+} ions are present. The creation of a charge-compensating vacancy and defect makes possible the transfer of electrons to the initially present Eu^{3+} ion, leading to the formation of Eu^{2+} ions. As a result only Eu^{2+} ions are present in 'as-grown' $KMgF_3$ crystal. The same is expected to occur for crystal growth using YbF_3 powder.

The ionic radii of Yb^{3+} and Yb^{2+} are 0.112 and 0.128 nm in the eightfold coordination, respectively, while the ionic radius of Ca^{2+} in the same coordination is 0.126 nm [38]. This means that the smaller Yb^{3+} ion is substituted for Ca^{2+} in CaF_2 more easily than the larger Yb^{2+} ion. The number of Yb^{3+} ions present during the crystal growth is much higher than the number of Yb^{2+} ions, since for the doping of Yb ions a mixture of YbF_3 and CaF_2 powders was used. This explains why not Yb^{2+} but Yb^{3+} ions are present in the 'as-grown' CaF_2 crystal.

4.2. Yb^{3+} absorption and luminescence bands

The Yb^{3+} ion gives rise to absorption bands due to the electronic transition from the $^2F_{7/2}$ ground state to the $^2F_{5/2}$ excited state in the 900–1050 nm spectral region. Several investigators reported absorption spectra of CaF_2 [7, 9, 13, 15, 40, 41], but unfortunately there are some discrepancies between their observations. For example, a band at about 922.0 nm reported by Low [13] and Voron'ko *et al* [7] was not observed by Kirton and McLaughlan [15]. Also the sharp and intense absorption band at 910.0 nm observed by Kiss [41] does not appear in the spectra of Voron'ko *et al* [7] and Low [13]. The two sharp Y1 and Y4 bands at 922.5 and 963.0 nm at 18 K observed for our 30% Yb^{3+} sample are also measured by Low [13] and Voron'ko *et al* [7], but not by Kiss [35].

The trivalent Yb^{3+} substitution gives rise to charge compensation, which originates from interstitial F^-. Depending on the location of the interstitial F^-, the Yb^{3+} ion has axial, trigonal

or orthorhombic symmetry [13]. When the interstitial F^- ions are located far from Yb^{3+}, cubic Yb^{3+} ions are created. The location of charge-compensating F^- ions depends on the Yb^{3+} concentration and crystal growth conditions. Kirton and McLaughlan [15] assigned various absorption bands, which appear in the 907–915 and 962–984 nm regions, to Yb^{3+} ions with cubic, tetragonal, trigonal and rhombohedral symmetries. Yb^{3+} ions with various site symmetries are created not only by the charge-compensating interstitial F^- ions but also by O^{2-}, OH^- and Na^+ ions in substitution, which are introduced unintentionally [13–15, 40]. Because the O^{2-} ionic radius is close to the F^- radius, O^{2-} ions are easily introduced and substituted for F^- ions. Thus, we can conclude that the different Yb^{3+} absorption spectra reported in the literature [7, 13–15, 35, 40, 41] are due to the different Yb^{3+} concentrations and different crystal growth conditions of the experiments, which give rise to the formation of many kinds of Yb^{3+} ions with different site symmetries in CaF_2.

The intensity of the Y1 band, which is due to Yb^{3+} with low symmetry, is comparable with that of the Y4 band. The $^2F_{7/2} \rightarrow {}^2F_{5/2}$ absorption band is caused by magnetic dipole and electric dipole forbidden transitions for Yb^{3+} ions with cubic and lower symmetries, such as cuboctahedral. Taking into account the effect of lattice vibration and lattice distortion on the cubic Yb^{3+}, the oscillator strength f-value of this band is expected to be much larger than the f-value of the pure magnetic dipole band [42, 43]. However, it is still much lower than the f-value of the electric dipole forbidden band due to the low symmetry Yb^{3+} ions. Therefore, the experimental results obtained suggest that the concentration of cuboctahedral Yb^{3+} ions is much higher than that of the cubic symmetry Yb^{3+} ions. This is inconsistent with the suggestion that 90–95% of Yb^{3+} ions are located on the cubic sites [15].

When 'as-grown' crystal containing Yb^{3+} ions was irradiated with γ-rays, the Yb^{3+} IR absorption spectra before and after irradiation were almost the same, and the Yb^{3+} band intensity was slightly decreased by the conversion to Yb^{2+} ions (as an effect of the Compton electron capture: $Yb^{3+} + e^- \rightarrow Yb^{2+}$). A reciprocal situation was observed for the crystals annealed in hydrogen. In their spectra, there was a clear decrease in the intensity of Yb^{3+} absorption that was confirmed by the lower intensity of Yb^{3+} emission that we observed.

Bearing in mind the results of absorption and photoluminescence measurements, we can conclude that quite different Yb^{2+} centres are created by γ-irradiation and annealing-in-hydrogen treatments. The latter favours Yb^{2+} isolated centres, probably located at Ca^{2+} sites, because the high temperature during annealing favours ordering of the CaF_2 lattice. The former favours Yb^{2+} centres related to Yb^{3+}, because Compton electrons can be easily captured by Yb^{3+} pairs usually present in Yb^{3+}-doped crystals, as was seen for our samples [9]. This conclusion is confirmed by the temperature dependence of the intensity of the 976.7 absorption line (Y5) ($1 \rightarrow 5$ transition in figure 8) that we also analysed. We distinguished at least two maxima at 150 and 220 K. They correspond to localized phonons with energies of 104 and 153 cm^{-1}, respectively. The same phonon bands were observed in the Raman spectra of the CaF_2:Yb crystals. The localized phonons may be related to Yb^{3+} pairs present in the crystal. Such a behaviour of the resonant line can be interpreted simply as an effect of non-radiative transfer between close Yb^{3+} ions by $^2F_{7/2} \leftrightarrow {}^2F_{5/2}$ zero-line resonant transition. We have previously observed this kind of temperature dependence for the Yb^{3+}-doped $LiNbO_3$ crystal [44].

Compared to the annealed crystal case, γ-irradiation does not change the position of the Yb^{3+} ion being converted to the Yb^{2+} one in the CaF_2 lattice. If prior to γ-irradiation, the Yb^{3+} ion was located within a cluster, it stayed there after γ-irradiation, but the cluster became recharged by capturing one Compton electron. In the case of annealing in hydrogen, the cluster is probably destroyed under the influence of temperature and the Yb^{3+} ion being converted to an Yb^{2+} one is shifted to the lattice Ca^{2+} position. This is confirmed by the isolated character

of the Yb^{2+} ion, as observed in the absorption spectrum of annealed-in-hydrogen crystal below 400 nm.

The observed EPR signal is assumed to be caused by the Yb^{3+}-or Yb^{3+}-associated centre since the Yb^{2+} ion with the f^{14} electron configuration is not responsible for the EPR signal although a precise assignment is difficult at this moment. The EPR signal decreases upon γ-irradiation. Such a behaviour is consistent with the assignment of the EPR signal because we propose that the Yb^{3+} to Yb^{2+} conversion occurs by the γ-irradiation.

The intensities of the Yb^{2+} UV absorption bands recorded after the γ-ray irradiation and H_2 annealing were comparable with those of Yb^{3+} IR bands. This can be explained by the fact that not all Yb^{3+} ions are converted to Yb^{2+} ions under these reduction methods. Only a small amount of Yb^{3+} ions are converted, i.e. a small amount of Yb^{2+} ions are created. The Yb^{2+} UV absorption bands are caused by the $f^{14} \rightarrow f^{13}d$ electric dipole allowed transition, while the Yb^{3+} IR bands come from $f^{13} \rightarrow f^{13}$ electric dipole forbidden but magnetic dipole allowed transitions, because a number of Yb^{3+} ions are located at cubic sites. Therefore, comparable absorption intensity was observed for the Yb^{2+} and Yb^{3+} bands even if the number of Yb^{2+} ions was much smaller than that of Yb^{3+} ions.

We observed a considerably intense and broad Y5 band ($1 \rightarrow 5$ in figure 8) in the 970–982 nm region. When the Yb^{3+} concentration is increased, several intense bands appear in this region [7]. Therefore, it is suggested that the presence of the intense 970–982 nm band is due to a high concentration of Yb^{3+} ions with different symmetries. The minimum Yb^{3+} concentration for our crystals was 0.5 at.%; however, it was still so high that we could not distinguish absorption bands due to the different site symmetry of Yb^{3+} in this region because of strong overlapping.

The observed IR Yb^{3+} absorption bands are broad and strongly overlap each other not only in the 970–982 nm regions but also in the other regions, resulting in a broad band with structure in the whole 900–1020 nm region, as can be seen in figures 1 and 7.

A quite different observation was made for the spectra of other rare-earth ions, such as Er^{3+}, Tm^{3+} and Nd^{3+}, which consist of sharp lines even at room temperature. Normally, the rare-earth ions exhibit atom-like sharp absorption and emission lines caused by inner core $f^n \rightarrow f^n$ electronic transitions. In the case of Yb^{3+} in CaF_2, many kinds of Yb^{3+} ions with different site symmetries are created and their $^2F_{5/2}$ excited levels are close to each other. As a result, a broad absorption band appears in a wide spectral region of 900–1020 nm.

As can be seen in figures 1 and 7, almost the same IR absorption spectra were obtained for the 'as-grown' crystals with 0.5, 5 and 30 at.% of Yb^{3+}, H_2-annealed crystal with 5 at.% of Yb^{3+} and γ-irradiated crystal with 30 at.% of Yb^{3+}. It is difficult to find clear differences in spectral line shape among these different crystals. However, the difference is more evident in the luminescence spectra, as shown in the inset of figure 11. If we could use crystals with much lower Yb^{3+} concentrations, i.e. about 0.1 at.%, it would be possible to see a difference in the absorption spectra, because well-resolved absorption bands can be observed in lightly doped crystals.

4.3. Yb^{2+} absorption bands

The A–G absorption bands appeared after the reduction procedure. From our present measurements it is suggested that the A, C, D and F bands belong to the same optical centre, i.e. the isolated Yb^{2+} centre. This is consistent with the experimental result of Loh [27]. In figure 10, we can see that the E band is different from the B and G bands. We consider that the E band is caused by Yb^{3+} ion with an Yb^{2+} neighbour (i.e. Yb^{3+}–Yb^{2+}) as suggested by Loh [28]. As to the B and G bands, we propose that they are caused by the Yb^{2+} ion accompanied by

an impurity such as a lattice vacancy or an unintentionally doped in OH^-, Na^+ or O^{2+} ion, because their intensities depend on the Yb^{3+} concentration, growth conditions and reduction procedure.

From the spectra obtained, we can see that the optical excitation into the E band gives rise to IR luminescence which is the same as Yb^{3+} luminescence. This can be explained as follows. An isolated Yb^{3+} ion (with the f^{13} electron configuration in the ground state) has higher energy levels due to the $f^{12}d$ configuration. These energy levels are located above 50 000 cm^{-1}, because the corresponding absorption is not observed at low energies below 50 000 cm^{-1} (200 nm in wavelength). When the Yb^{2+} ion is located close to Yb^{3+}, the $f^{12}d$ energy levels of Yb^{3+} become low, giving rise to the E absorption band at 238 nm. Thus, the excitation into the E band results in excitation of Yb^{3+}, leading to Yb^{3+} luminescence.

The Yb^{3+} luminescence is also observed upon excitation in the A, C, D and F bands due to isolated Yb^{2+} (see figure 11). Pedrini *et al* [19] reported photoconductivity in Tm^{2+}-, Dy^{2+}- and Ho^{2+}-doped CaF_2. Tm^{2+} is isoelectronic with Yb^{3+}. In CaF_2, Tm^{2+} has $f^{13} \rightarrow f^{12}d$ absorption bands at about 585, 445, 408 and 345 nm [25]. The photoconductivity of Tm^{2+}-doped CaF_2 is observed at high energy above 450 nm and its intensity increases with increasing photon energy [19]. Taking into account these results, we suggest that the excitation in the A, C, D and F absorption bands of Yb^{2+} gives rise to photo-ionization of Yb^{2+} ions and electrons in the conduction band to form excited Yb^{3+} ions which emit IR Yb^{3+} luminescence. As can be seen in figure 11, the excitation spectrum for the 980 nm emission is not similar to the A–F absorption spectrum. For example, the excitation peak intensities of A and C bands are much weaker than that of the D band. This is due to the fact that the photoconductivity is less effective for the low energy absorption bands [19]. This confirms our above-mentioned suggestion that the A, C, D and F bands are caused by isolated Yb^{2+}.

Unlike the cases of various host materials where the Yb^{2+} luminescence was reported even at room temperature [29, 45], for CaF_2 it has been observed below 200 K [10, 46]. According to Rubio [29], the Yb^{2+} luminescence spectrum consists of a structureless broad band in the yellow-green region with a superposition of two overlapping bands peaking at 17 600 cm^{-1} (568 nm) and 18 200 cm^{-1} (549 nm). We excited γ-irradiated CaF_2:30 at.% Yb^{3+} crystal with 357 nm light (i.e. A band excitation) at room temperature, and obtained a considerably weak emission band at about 565 nm with a shoulder at about 540 nm. This 565 nm band seems to correspond to the 568 nm band mentioned by Rubio [29], while the 540 nm shoulder corresponds to the 549 nm band. This indicates that, although the yellow-green luminescence associated with Yb^{2+} is intense below 200 K [10, 46], it still appears very weakly even at room temperature.

5. Conclusions

The observed IR Yb^{3+} absorption bands are broad and strongly overlap each other not only in the 970–982 nm regions but also in other regions, resulting in a broad band with structure in the whole 900–1020 nm region. In the absorption spectra of both γ-irradiated and annealed-in-hydrogen CaF_2:Yb^{3+} crystals, Yb^{3+} ions with at least cubic and cuboctahedral site symmetries were observed. The results observed suggest that the concentration of cuboctahedral Yb^{3+} ions is much higher than that of the Yb^{3+} ions with cubic symmetry. For the H_2-annealed crystal, A, B, C, D, F and G bands are observed below 400 nm. They are assigned to Yb^{2+}-and Yb^{2+}-associated centres. The H_2-annealed CaF_2:Yb^{3+} crystals reveal luminescence bands in the 950–1100 nm region upon excitation with UV light. From the study of the UV absorption spectrum of γ-irradiated CaF_2:5 at.% Yb^{3+} crystal, the assignment for the A–G bands is confirmed.

The low temperature (18 K) IR absorption spectra of the γ-irradiated CaF_2:30 at.% Yb^{3+} crystal reveal the Y1, Y3, Y4 and Y5 absorption bands. With increasing temperature, the intensities of the Y1 and Y3 bands decrease, while the Y4 band shifts to lower energy, and new Y2, Y6 and Y7 absorption bands appear. Such temperature-sensitive Y2, Y6 and Y7 bands are attributed to the hot bands. The sharp Y4 band is suggested to be due to the cuboctahedral Yb^{3+} site while the Y1 and Y3 bands are attributed to phonon side bands.

From the present study it is suggested that only a negligible amount of Yb^{3+} ions are converted into Yb^{2+} under the γ-irradiation. The presence of Yb^{2+} is confirmed by the 565 and 540 nm luminescence under 357 nm excitation. It is also suggested that the excitation in the A, C, D and F absorption bands of Yb^{2+} gives rise to photo-ionization of Yb^{2+} ions and electrons in the conduction band to form the excited Yb^{3+} ions which emit IR Yb^{3+} luminescence.

Differences in structure of UV absorption and emission spectra are observed between the γ-irradiated crystals and the crystal annealed under hydrogen, suggesting that different mechanisms are responsible for the creation of Yb^{2+} ions under γ-irradiation and annealing in hydrogen. The latter favours Yb^{2+} isolated centres that may be located at Ca^{2+} sites, because the high temperature during annealing favours ordering of the CaF_2 lattice. The former favours Yb^{2+} centres related to Yb^{3+}, because electrons can be easily captured by Yb^{3+} pairs usually present in Yb^{3+}-doped crystals. This conclusion is confirmed by the observed temperature dependence of the intensity of the 976.7 resonant absorption line (Y5 or $1 \rightarrow 5$).

Acknowledgments

We would like to thank Professor Tsuguo Fukuda for giving us the opportunity to grow Yb^{2+}-doped CaF_2 crystals by simple melting in his Laboratory at the Tohoku University, Sendai, Japan, and to MSc Maksymilian Włodarski from the Institute of Optoelectronics, Military University of Technology, Warsaw, Poland, for absorption and photoluminescence measurements.

References

[1] De Loach L, Payne S A, Chase L L, Smith L K, Kway W L and Krupke W F 1993 *IEEE J. Quantum Electron.* **29** 1179
[2] Brenier A and Boulon G 2001 *Europhys. Lett.* **55** 647
[3] Brenier A and Boulon G 2002 *J. Alloys Compounds* **323/324** 210
[4] Bourdet G L 2001 *Opt. Commun.* **198** 411
[5] Kuck S 2001 *Appl. Phys.* B **72** 515
[6] Baker J M 1974 *Crystals With The Fluorite Structure* ed W Hayes (Oxford: Clarendon) p 341
[7] Voron'ko Yu K, Osiko V V and Shcherbakov I A 1969 *Sov. Phys.—JETP* **29** 86
[8] Yoshikawa A, Boulon G, Laversenne L, Canibano H, Lebbou K, Collombet A, Guyot Y and Fukuda T 2003 *J. Appl. Phys.* **94** 5479
[9] Ito M, Goutaudier C, Lebbou K, Guyot Y, Fukuda T and Boulon G 2003 *Physica* B at press
[10] Kaplyanskii A A, Medvedev V N and Smolyanskii P L 1976 *Opt. Spectrosc.* **41** 615
[11] Reut E G 1976 *Opt. Spectrosc.* **40** 55
[12] Lizzo S, Meijerink A, Dirksen G J and Blasse G 1995 *J. Lumin.* **63** 223
[13] Low W 1962 *J. Chem. Phys.* **37** 30
[14] McLaughlan S D and Newman R C 1965 *Phys. Lett.* **19** 552
[15] Kirton J and Mclaughlan S D 1967 *Phys. Rev.* **155** 279
[16] Ranon U and Hyde J S 1966 *Phys. Rev.* **141** 259
[17] Kirton J and White A M 1969 *Phys. Rev.* **178** 543
[18] Kuhner D H, Lauer H V and Bron W E 1972 *Phys. Rev.* B **5** 4112
[19] Pedrini C, McClure D S and Anderson C H 1979 *J. Chem. Phys.* **70** 4959
[20] Ignatev I V and Ovsyankin V V 1977 *Opt. Spectrosc.* **43** 644

[21] Cohen E and Guggenheim H J 1968 *Phys. Rev.* **175** 354
[22] Piper T S, Brown J P and McClure D S 1967 *J. Chem. Phys.* **46** 1353
[23] O'Connor J R and Bostick H A 1962 *J. Appl. Phys.* **33** 1868
[24] Macfarlane R M, Brocklesby W S, Bloch P D and Harley R T *Opt. Commun.* **58** 25
[25] McClure D S and Kiss Z 1963 *J. Chem. Phys.* **39** 3251
[26] Kaplyanskii A A and Feofilov P P 1962 *Opt. Spectrosc.* **13** 129
[27] Loh E 1968 *Phys. Rev.* **175** 533
[28] Loh E 1969 *Phys. Rev.* **184** 348
[29] Rubio J O 1991 *J. Phys. Chem. Solids* **52** 101
[30] Tsuboi T, Witzke H and McClure D S 1981 *J. Lumin.* **24/25** 305
[31] Cantelar E, Sanz-Garcia J A and Cusso F 1999 *J. Cryst. Growth* **205** 196
[32] Foulon G, Ferriol M, Brenier A, Cohen-Adad M T and Boulon G 1995 *Chem. Phys. Lett.* **245** 555
[33] Montoya E, Lorenzo A and Bausa L E 1999 *J. Phys.: Condens. Matter* **11** 311
[34] Hayes W and Stoneham A M 1974 *Crystals With The Fluorite Structure* ed W Hayes (Oxford: Clarendon) p 185
[35] Scacco A, Grassano U M, Francini R and Zema N 1998 Luminescent rare earth impurities in $KMgF_3$ crystals *Proc. 9th CIMTEC World Forum on New Materials, Symp. X—Innovative Light Emitting Materials (Florence, Italy)* ed P Vincenzini and G C Righini
[36] Tsuboi T and Scacco A 1998 *J. Phys.: Condens. Matter* **10** 7259
[37] Francini R, Grassano U M, Boiko S, Tarasov G G and Scacco A 1999 *J. Chem. Phys.* **110** 457
[38] Shannon R D 1976 *Acta Crystallogr.* A **32** 751
[39] Seo H J, Moon B K and Tsuboi T 2000 *Phys. Rev.* B **62** 12688
[40] Falin M L, Gerasimov K I, Latypov V A, Leushin A M, Bill H and Lovy D 2003 *J. Lumin.* **102/103** 239
[41] Kiss Z 1962 *Phys. Rev.* **127** 718
[42] Sugano S, Tanabe Y and Kamimura H 1970 *Multiplets of Transition-Metal Ions in Crystals* (New York: Academic) chapter 5
[43] Henderson B and Imbush G F 1989 *Optical Spectroscopy of Inorganic Solids* (Oxford: Oxford Science) chapter 4
[44] Kaczmarek S M, Tsuboi T, Boulon G, Wabia M, Włodarski M, Pracka I, Podgórska D, Czuba M and Warchoł S 2004 *Mol. Phys. Rep.* **39** 99–114
[45] Tsuboi T, McClure D S and Wong W C 1993 *Phys. Rev.* B **48** 62
[46] Witzke H, McClure D S and Mitchell B 1973 *Luminescence of Crystals, Molecules and Solutions* ed F Williams (New York: Plenum) p 598